

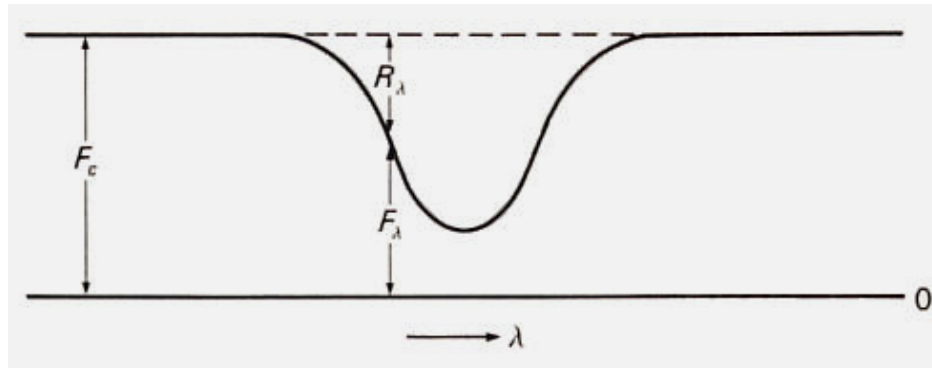
4 - Analysis of spectral lines

This chapter is dedicated to an elementary analysis of the spectral lines seen in absorption in the spectra of normal stars.

Many figures and information have been taken from the literature quoted in the References in appendix to previous chapters.

The line profile

Suppose we have at our disposal a well calibrated spectrum, with reciprocal dispersion high enough to discern strong and weak absorption lines, and to measure with precision the line profile F_λ (after removing the instrumental effects), as in the figure.



We can call *line depth* (or residual intensity) R_λ the a-dimensional quantity:

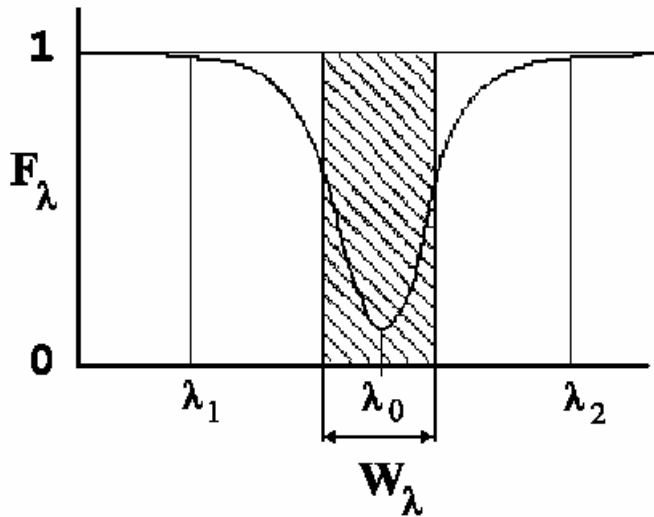
$$R_\lambda = \frac{F_c - F_\lambda}{F_c} = 1 - \frac{F_\lambda}{F_c}$$

which varies between 0 (a very weak line) to 1 (a very deep, almost saturated) line.

The equivalent width

Normalize then to $F_c = 1$ and calculate the total integrated and normalized intensity A_{λ_0} .

$$A_{\lambda_0} = \int_{\lambda_1}^{\lambda_2} (1 - F_{\lambda}) d\lambda = \int_{\lambda_1}^{\lambda_2} R_{\lambda} d\lambda$$

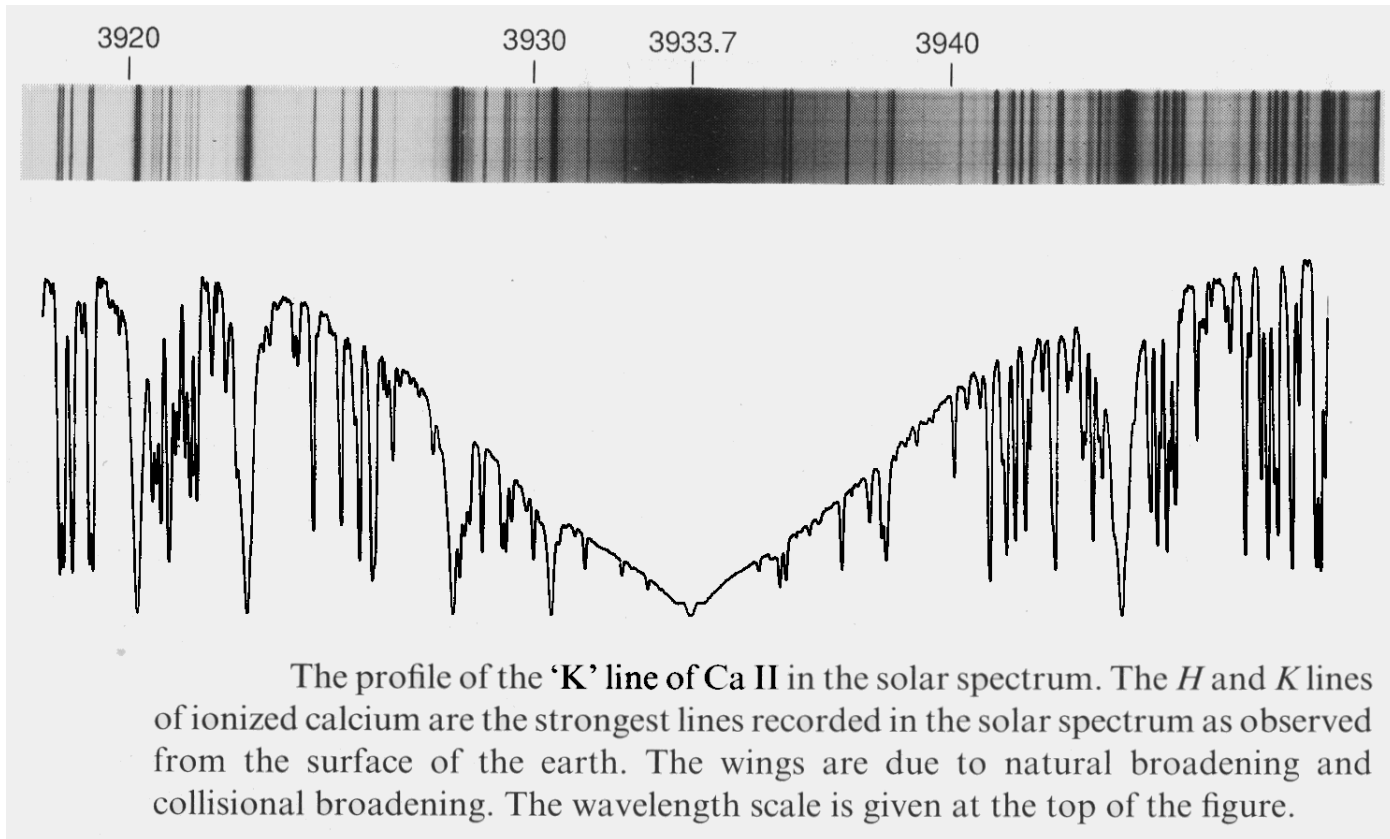


A widely used parameter is the so-called *equivalent width* W_{λ_0} of the line, namely the width (usually in Å, or mÅ) of a rectangle having the same total integrated energy A_{λ_0} as the true line.

The terms *equivalent width* and *intensity* are often used as synonyms. Notice that the equivalent width alone *does not discriminate between a shallow wide line and a narrow deep one.*

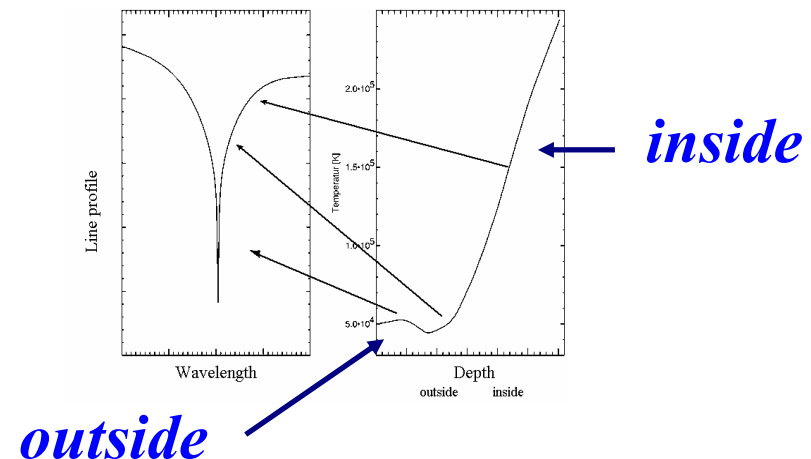
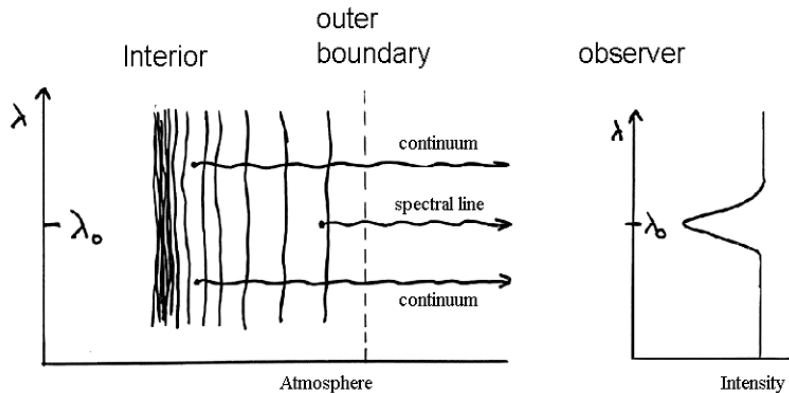
Practical problems

The determination of the continuum level *is not always easy*, as in this example to the solar Ca II K line taken at high resolution:

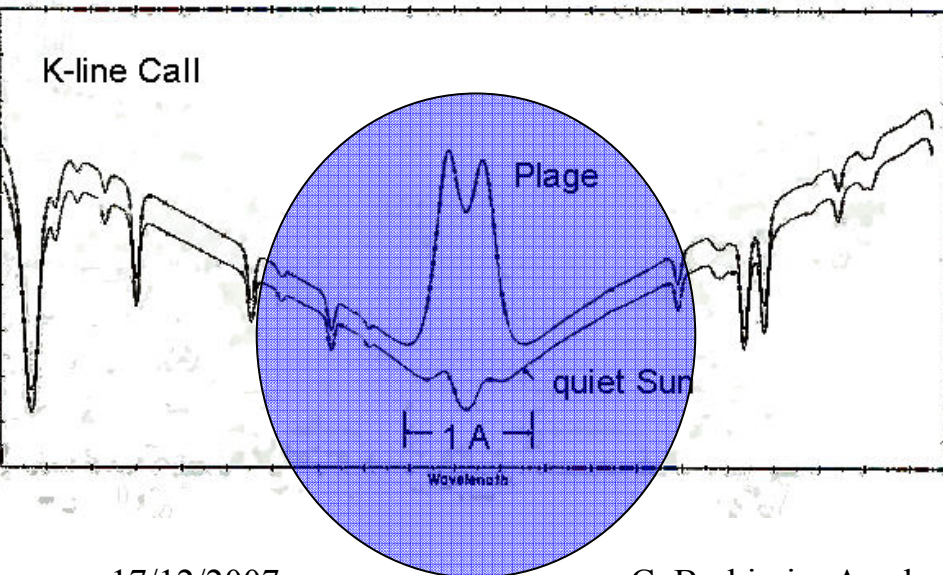
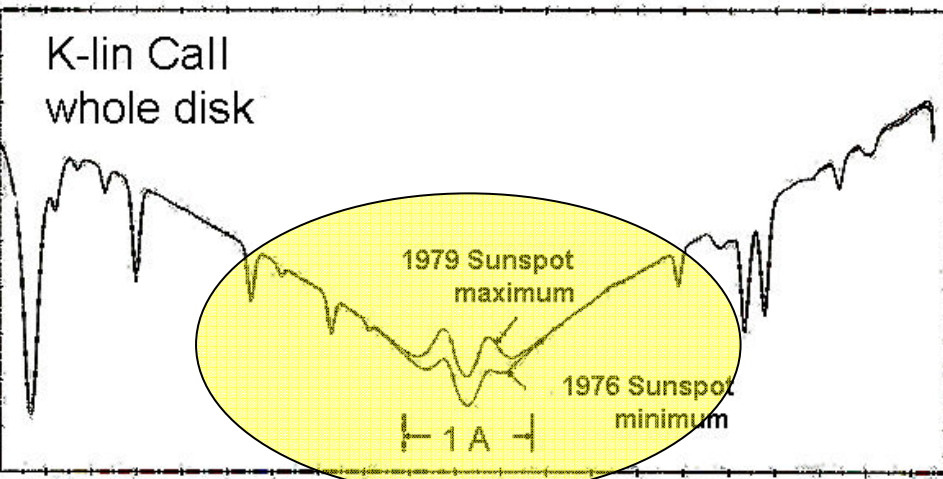


Where absorption lines form - 1

Let us recall that the different parts of the line profile derive from different *geometrical* depths, according to the different *optical* depths. The core of the line comes from the region of lower, the wings from the regions of higher optical depths: the temperature drops towards the outside, therefore in general *the core will generate in outer regions of lower temperature, the wings in inner regions of higher temperature*, as schematically indicated in the figure.



Where absorption lines form - 2



Due to their high opacity, the cores of the Ca II lines can come directly from the chromosphere.

Upper panel: spectrum of the *whole disk* in 1976 (minimum activity, or *quiet sun*) and 1979 (maximum activity). At the very bottom of the line, an emission tends to be seen (*line reversal*).

Lower panel: the slit of the spectrograph isolates a very active region (a so-called *plage*), where the reversal is quite obvious, nevertheless the absorption can still be seen.

Notice that very high spectral resolution is needed to detect the reversal.

Effect of absorption lines on $T(z)$ - 1

We might call this effect also as ‘*influence of non-greyness on temperature stratification*’.

Recall that for the grey atmosphere we found:

$$T^4 = \frac{3}{4} T_{\text{eff}}^4 [\tau_R + q(\tau_R)] \quad \tau_R = \text{Rosseland mean value of } \tau_\lambda$$

When there are strong absorption lines, part of the energy is scattered back into the lower atmosphere: where κ_λ is large (strong line) the intensity I_λ and the flux F_λ decrease.

Therefore, if we had the same temperature stratification of the grey case. the effective temperature would decrease:

if we want to conserve the total flux, the temperature of the continuum (where κ_λ is small) ***must increase***.

Effect of absorption lines on $T(z)$ - 2

Let us try a modified temperature stratification of the form:

$$T^4 = \frac{3}{4} T'_{\text{eff}}{}^4 [\bar{\tau} + q(\bar{\tau})] \quad \bar{\tau} = \text{some mean value of } \tau_\lambda$$

which leads to a flux:
$$\int_0^\infty \pi F_\lambda d\lambda = \pi F = \sigma T'_{\text{eff}}{}^4 (1 - \eta)$$

where η is the total fraction of continuum removed by the lines.

Then, if we impose:
$$\pi F = \sigma T_{\text{eff}}{}^4$$

we must also have:
$$T_{\text{eff}}{}^4 = T'_{\text{eff}}{}^4 (1 - \eta) \quad , \quad T'_{\text{eff}} = T_{\text{eff}} / (1 - \eta)^{1/4}$$

Effect of absorption lines on $T(z)$ - 3

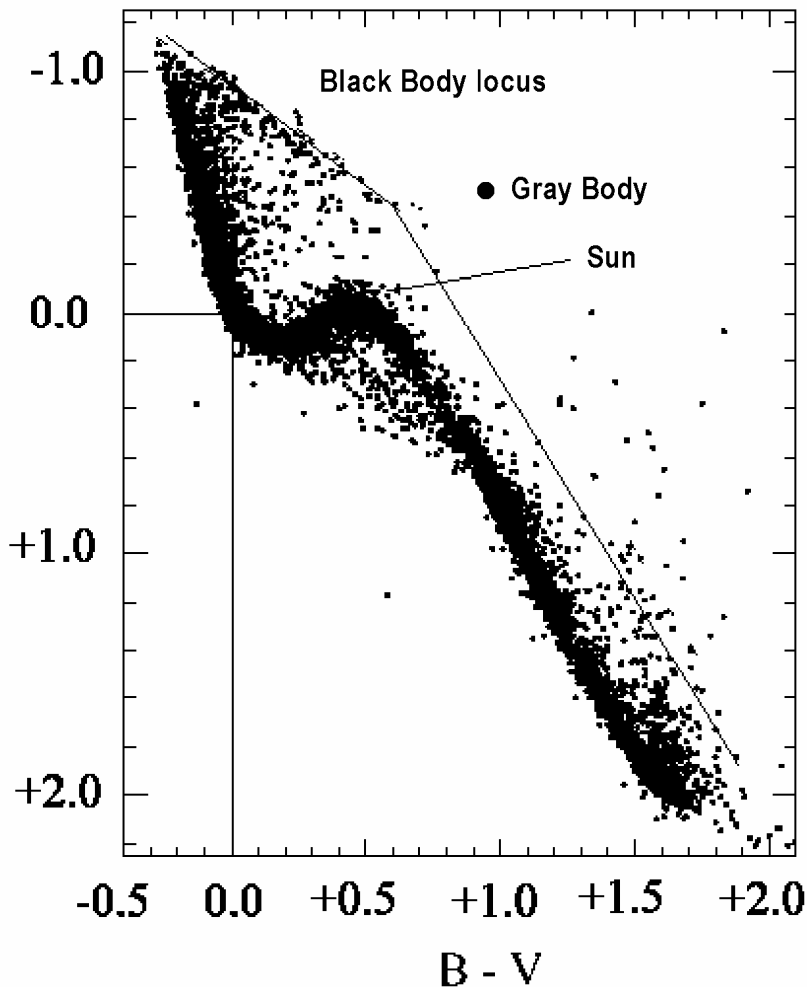
In the case of the Sun, $\eta \approx 14\%$, so that:

$$T'_{\text{eff}} \approx T_{\text{eff}} / (0.84)^{1/4} = (1 + 0.035)T_{\text{eff}}$$

The temperature of the Sun in the continuum (namely the *color temperature*) must be approximately **200 K higher than the effective temperature**.

Notice that in general the effect **will depend on the chemical composition, but also on the pressure (luminosity class, radius)**, because of Saha equation.

Effect of absorption lines on two-color diagrams



We recall that *two color diagrams*, such as (U-B , B-V), are affected by the absorption lines.

Different *line-blanketings*, caused for instance by a different content of metals, move the position of the star in the diagram. This effect is particularly seen in the U-band, and causes a *UV-excess in metal poor stars*.

Other photometric systems (e.g. Stromgren's) are even more sensitive to spectral lines and Balmer discontinuities.

Factors affecting W_λ

We expect that the equivalent width W_λ depends on the **number of atoms N in the atmosphere** capable to absorb that transition, therefore on the *temperature and density* (or pressure) inside the gas, and on the *chemical composition* of the star (*number of atoms* in the present context means the total number of those atoms in the column of unit cross-section).

Furthermore, the strength of a given line will depend **on atomic properties**, summarized by the f factor previously discussed, and which we assume known a priori (not always true!).

The theory shows that we need to consider W_λ as function of the product $N \cdot f$:

$$W_\lambda = W_\lambda(N \cdot f)$$

This relationship is **far from linear**, and critically depends not only on the density but also on the *broadening mechanisms* affecting the line, as we now discuss.

The natural width - 1

The *minimum possible* width is the *natural width* of the line (recall the Heisenberg principle) *plus eventually the hyperfine structure due to isotopes* (which for the moment we leave aside). We have seen that this minimum width in the visible is of the order of $0.0001 - 0.001 \text{ \AA}$.

To determine the line profile, we can make recourse to the semi-classical radiation theory of an accelerated charge:

$$\frac{dW}{dt} = -\frac{2e^2\omega^2}{3mc^3}W = -\gamma W \quad , \quad \gamma = 0.22 / \lambda^2 \quad (\lambda \text{ in cm})$$

where m and e are mass and charge of the electron.

This result can be converted to the quantum mechanical result by making use of Einstein probability coefficient A for that particular transition.

The natural width - 2

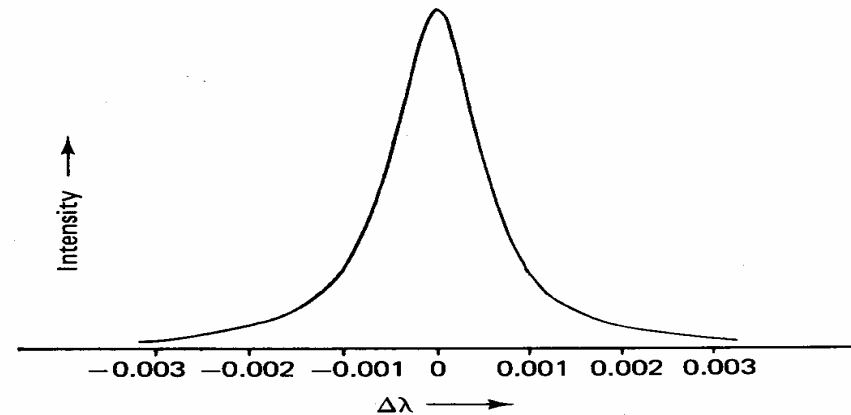
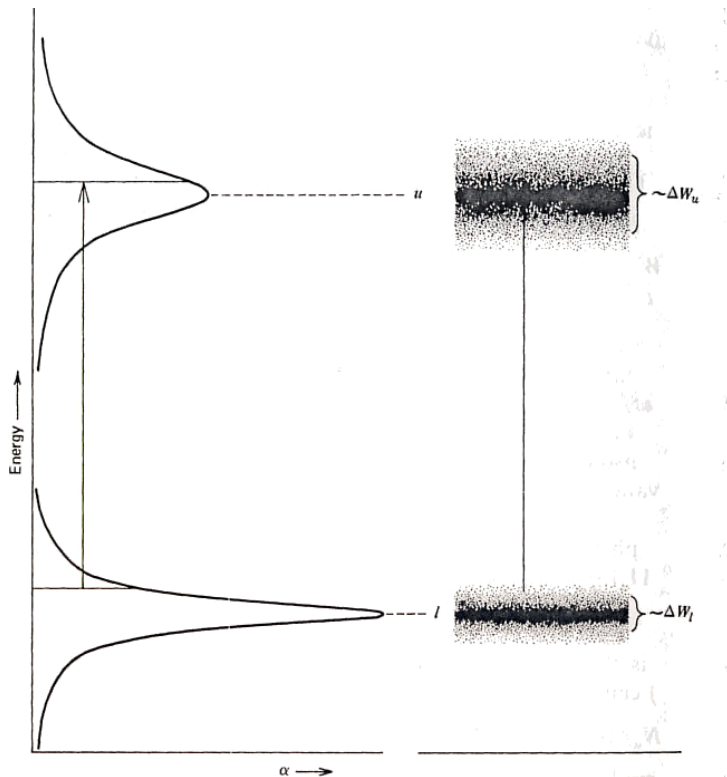
Converting the Einstein coefficient A to oscillator strengths f , the linear absorption coefficient becomes:

$$\kappa_{\omega} \approx \text{const} \frac{\gamma}{\left[(\omega - \omega_0)^2 + \gamma^2 / 4 \right]} f \quad , \quad \gamma = \frac{2e^2}{3mc\lambda_0^2}$$

where ω_0 is the central frequency and λ_0 the central wavelength of the line, f the oscillator strength of the transition. The **damping constant** γ represents also the Full Width Half Maximum (FWHM) of the line.

This profile is called **damping**, or **Lorentzian**, or **Cauchy**, profile. Notice that according to the system of units (e.g. mks instead of cgs) a factor 4π might appear in the definition of γ .

The natural width - 3

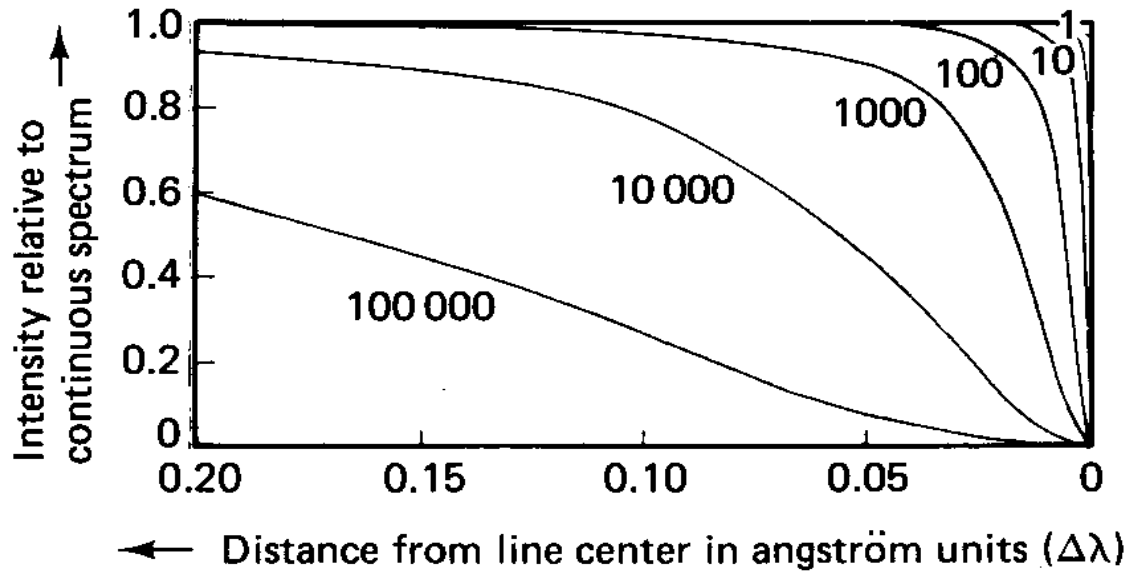


Schematics of energy level widths.

The upper level is usually much broader than the lower level.

This example pertains to the 4383Å line of FeI atoms cooled to liquid He temperatures. Notice that the wings of the line are faint *but extend to large distance from the core*.

Observed widths - 1



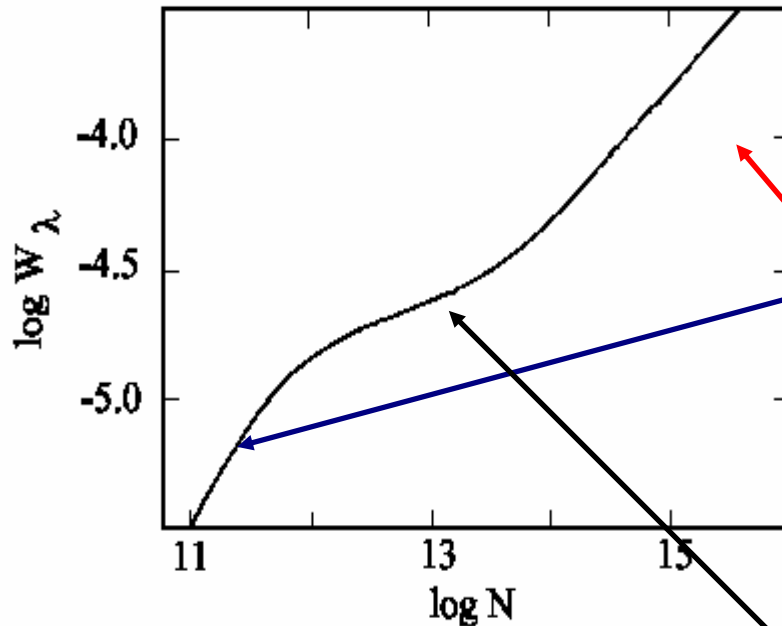
The observed widths are usually much larger than the natural ones, and *depend on the gas density*, as schematically shown in the above figure, where the ordinate is the intensity of the absorption relative to the continuum, 0 means total absorption, 1 no absorption: it is seen that the profile considerably *broadens* when the number of absorbing atoms in the column increases from 1 to 100000.

Observed widths - 2

From the previous figure we see that the absorptivity of the gas is *always very high at the center of the line*, dropping to almost zero with increasing distance from it:

- a small number of atoms will produce a strong absorption at the very center of the line, and almost no wings: the line will be deep and very narrow.

- by increasing the number of atoms, the *wings will gradually grow*.



Observations and theory show that the equivalent width regime passes *from a linear dependence at low densities*:

$$W = Nf$$

to a much slower one at higher column densities, essentially as:

$$W = \sqrt{Nf}$$

Notice the intermediate plateau at almost constant intensity.

Observed widths - 3

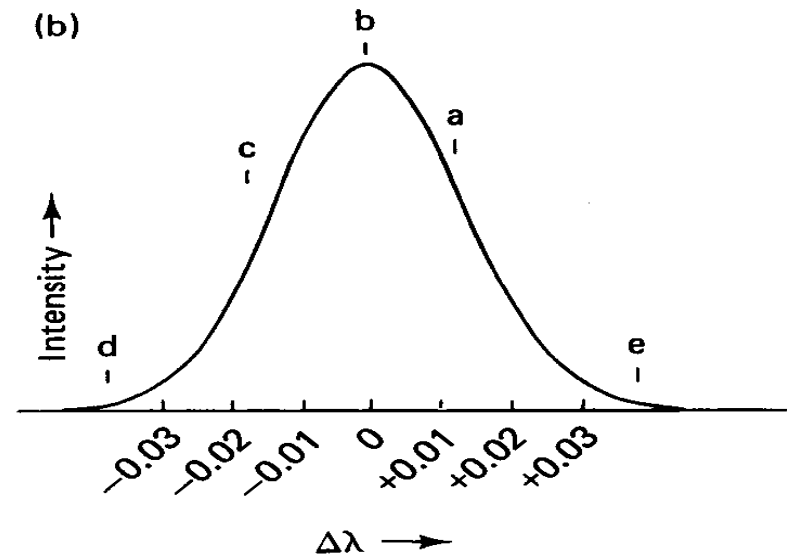
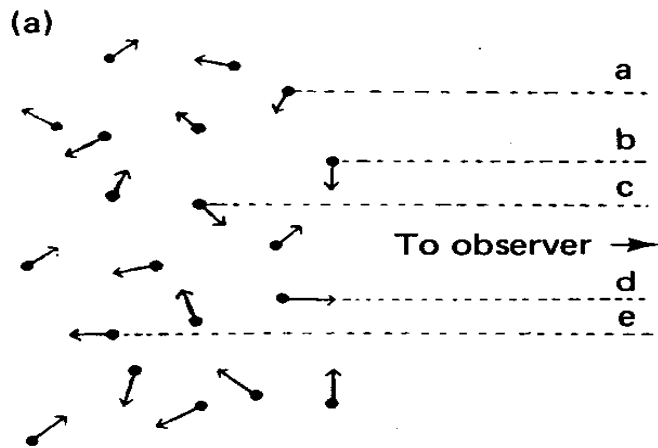
We must conclude that, while the natural width (and hyperfine structure due to isotope splitting, the effect is greatest for hydrogen, e.g. deuterium vs hydrogen). usually do not contribute more than few mÅ in the visible region, *other macroscopic effects will dominate the observed profiles.*

Such effects are *thermal Doppler* broadening, *collisional* broadening (which is better discussed in later slides), and possibly other effects (e.g. *Zeeman* effect if a magnetic field is present, the *rotation* of the star, *large scale currents*, etc.).

Thermal agitation (Doppler)

An important cause of broadening is the **thermal agitation**, namely the *superposition of the individual Doppler shifts*.

The figure shows the profile of the 4383 Å line of FeI when heated to 5700K as in the solar photosphere. The letters (a) to (e) pertain to the atoms moving as in the left side of the figure.



Broadening by thermal agitation (Doppler)

What matters in this discussion is the velocity \mathbf{V} of particles of mass m , *along the line of sight*, which we assume (not necessarily true) given by Maxwell law, with a maximum at \mathbf{V}_0 :

$$V_0 = \sqrt{\frac{2kT}{m}}$$

Each particle will absorb at larger or smaller wavelengths according to its velocity. The line profile is given by a *Gaussian function*:

$$I_\lambda = I_0 e^{-(\Delta\lambda/\Delta\lambda_D)^2}, \quad \Delta\lambda_D = \frac{\lambda}{c} V_0 = \frac{\lambda}{c} \sqrt{\frac{2kT}{m}}$$

The profile is broader when the kinetic temperature is higher.

The lines of the lighter elements, in particular hydrogen, will therefore be the widest.

Doppler FWHM

The Doppler FWHM is given by:

$$\text{FWHM} = 1.665 \Delta\lambda_D = \text{const} \cdot \lambda \sqrt{\frac{T}{m}}$$

The value of the constant depends on the units of λ .

Using the atomic mass M instead of m , we derive the temperature from the measured FWHM from:

$$T = 1.95 \times 10^{12} M \left(\frac{\text{FWHM}}{\lambda(\text{A})} \right)^2$$

Other Formulae for Doppler profile

The **Gaussian** line profile $\phi(\nu)$ can be expressed in terms of the Doppler width as:

$$\phi(\nu) = \frac{B}{\exp[(\nu - \nu_0)^2 / \Delta \nu_D^2]}$$

where B is a constant, m is the mass, μ the atomic mass, and the maximum is at ν_0 .

The width of the curve is:

$$\Delta \nu_D = \frac{\nu_0}{c} \sqrt{\frac{2kT}{m}} = \frac{1}{\lambda_0} \sqrt{\frac{2kT}{m}} = 1.285 \times 10^{11} \frac{1}{\lambda_{0(\text{nm})}} \sqrt{\frac{T(K)}{\mu}}$$

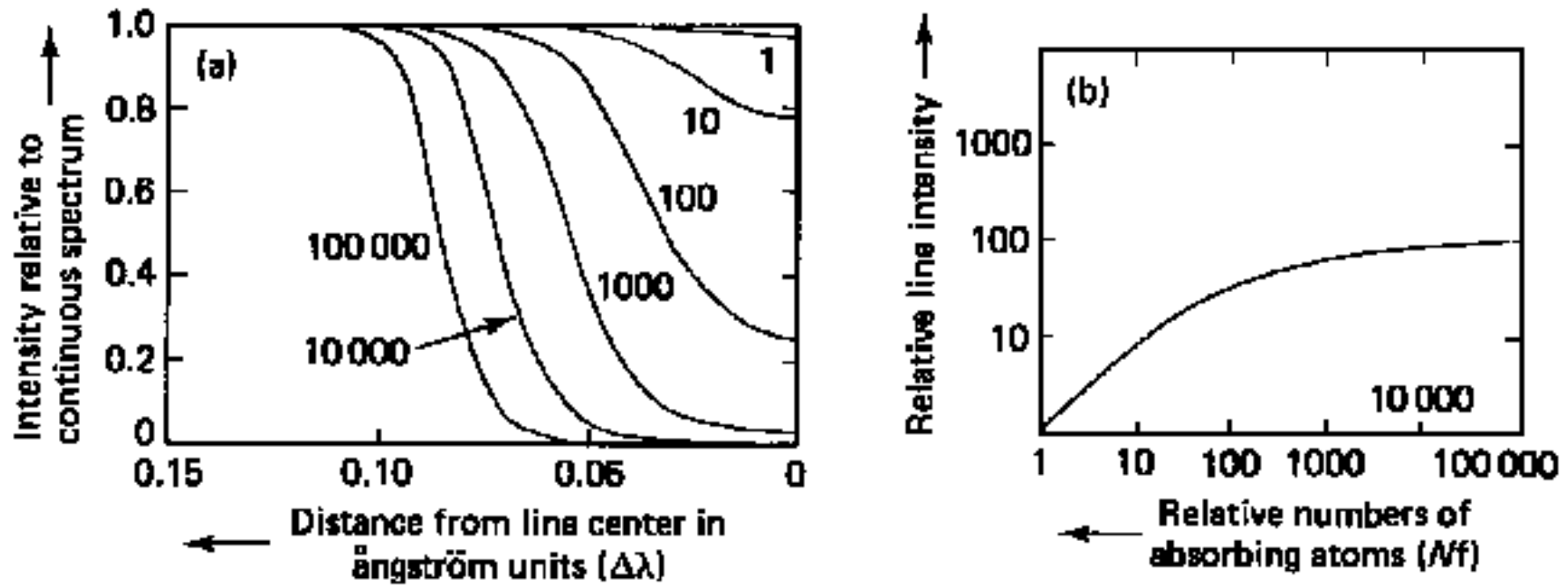
if λ_0 is measured in nm. The FWHM $\Delta \nu_{1/2}$ is connected to $\Delta \nu_D$ by:

$$\Delta \nu_{1/2} = 2(\nu_1 - \nu_0) = 2\Delta \nu_D \sqrt{\ln 2} = 2.139 \times 10^{11} \sqrt{(T / \mu)} / \lambda_0$$

In wavelength units:

$$\Delta \lambda_{1/2} = \frac{\lambda_0^2}{c} \Delta \nu_{1/2}$$

Doppler broadening and number of atoms



- a) Pure Doppler broadening; the intensity increases very slowly with the number of atoms and tends **to saturate the core**.
- b) Another way of showing the **saturation effect**, increasing the number of atoms beyond a certain value does not increase the intensity of the line.

Example - 1

For the Sun, with $T \sim 6000\text{K}$ at $\text{H}\alpha$ (6563°):

$$\Delta \nu_{1/2} = 2.139 \times 10^{11} \sqrt{(T / \mu)} / \lambda_0 = 2.139 \times 10^{11} \sqrt{(6000 / 1)} / 656.2 = 25.2 \text{ GHz}$$

i.e. in wavelength units:

$$\Delta \lambda_{1/2} = \frac{\lambda_0^2}{c} \Delta \nu_{1/2} = \frac{(6.56 \times 10^{-7})^2}{3 \times 10^8} 25.2 \times 10^9 = 0.36 \text{ \AA}$$

In velocity units:

$$\Delta u_{1/2} = c \frac{\Delta \lambda_{1/2}}{\lambda_0} = 3 \times 10^8 \frac{0.36}{6562} = 16.5 \text{ km/s}$$

This Doppler width is thus much larger than the natural damping width of the line (10^{-4} \AA), but nevertheless it is much smaller than the Stark pressure broadening we discuss in a moment.

Example - 2

The atomic mass dependence in the denominator implies smaller line widths for metallic lines, e.g. a factor of $(56)^{1/2}$ smaller for iron lines.

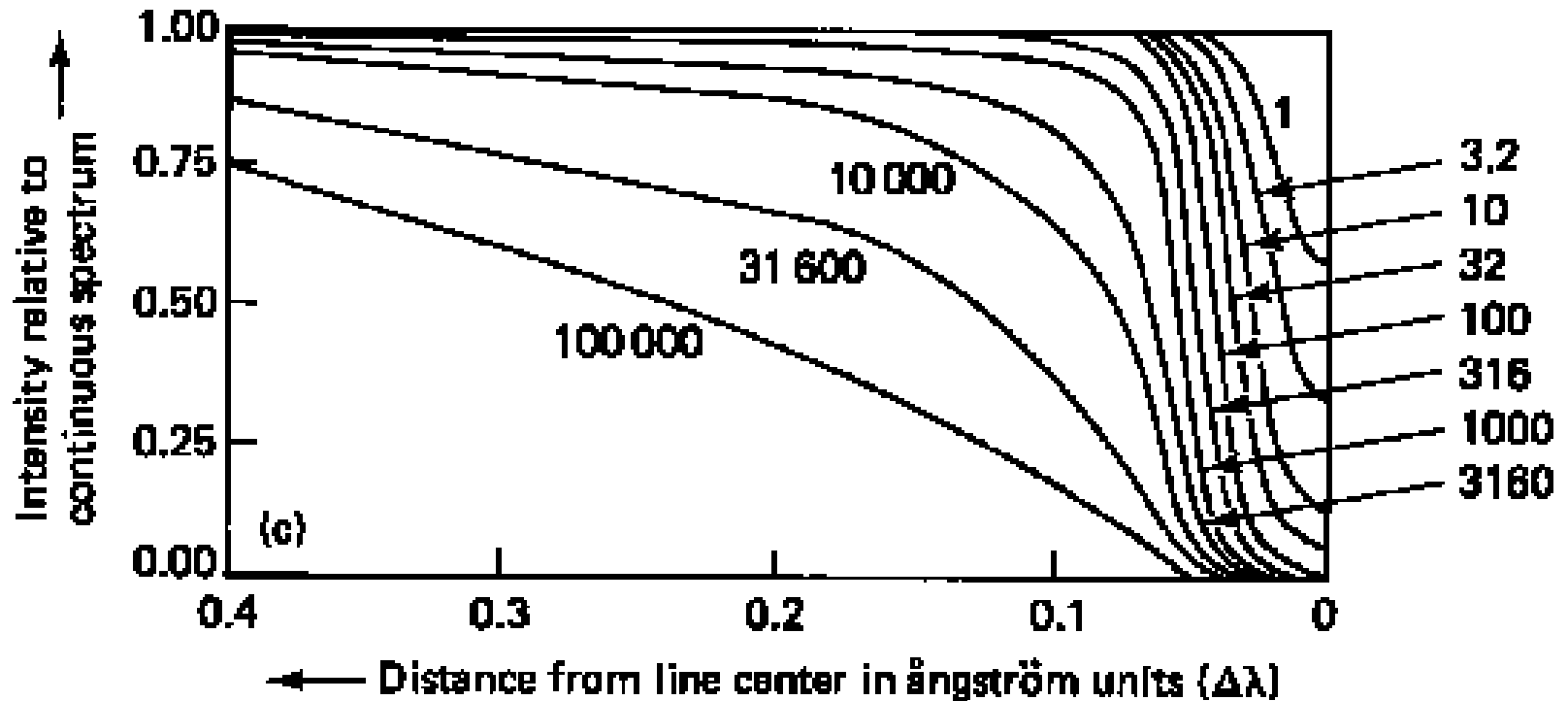
So, let us consider the coronal line 5303 [FeXIV]. The measured FWHM is 0.8\AA .

We easily find that the kinetic energy of Fe XIV in the corona corresponds to a temperature of 2.8 MK.

Superposition of the various effects: the Voigt profile

- Generally, we have to consider both the Doppler and damping profiles.
- The damping profile is negligible in the line core, but the Doppler profile decreases very steeply in the wings, whilst the damping profile decreases only as $1/\Delta\lambda^2$
- The final form of the combined profile (*Voigt profile*) depends on a parameter α , namely on the ratio of the damping widths $\gamma/2$ to the Doppler width $\Delta\nu_D$: $\alpha = \gamma / (2 \cdot \Delta\nu_D)$
- As a rule of thumb, the damping wings start to contribute a distance $-(\log \alpha)\Delta\lambda_D$ from the line centre.

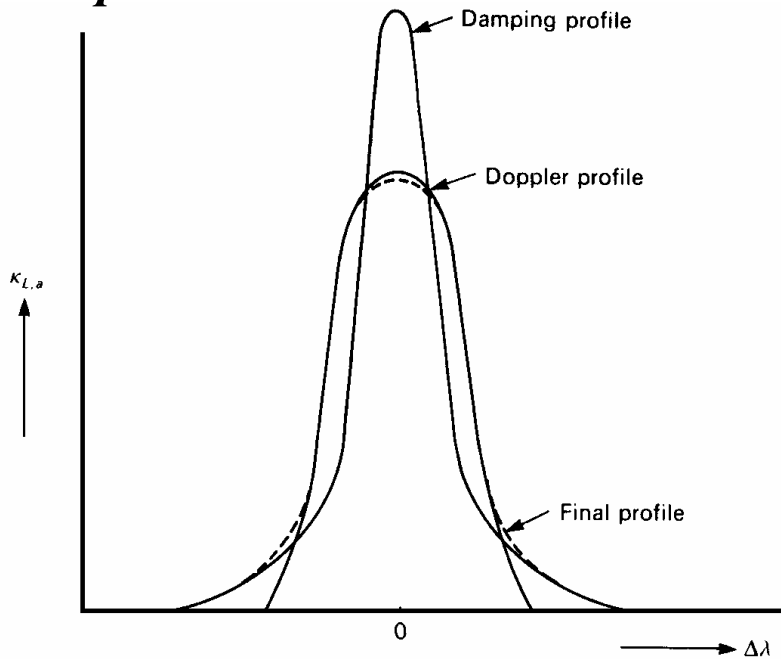
Doppler plus Natural Broadening



c) Combination of Doppler plus natural; at the beginning (low number of atoms), the profile resembles that of the Doppler profile alone.

Voigt Profile

careful: the stellar lines are in absorption!



While the *Doppler* broadening is more efficient at the center of the line, the *natural width* (and also the *collisional* damping we'll discuss in a moment) contribute more to the wings. The resultant profile is expressed by Voigt's function $V(\gamma, \nu)$ which is the convolution of a Lorentzian with a Gaussian:

$$V(\gamma, \nu) = \frac{\gamma}{\pi} \int_{-\infty}^{+\infty} \frac{e^{-x^2}}{\gamma^2 + (\nu - x)^2} dx, \quad \nu = \Delta\lambda / \Delta\lambda_D, \quad \gamma = \gamma_{\text{rad}} + \gamma_{\text{coll}}$$

Numerical methods are needed for the calculation of the function V .

Summary of overall effect on $W_\lambda - 1$

Summarizing the previous (oversimplified) discussion:

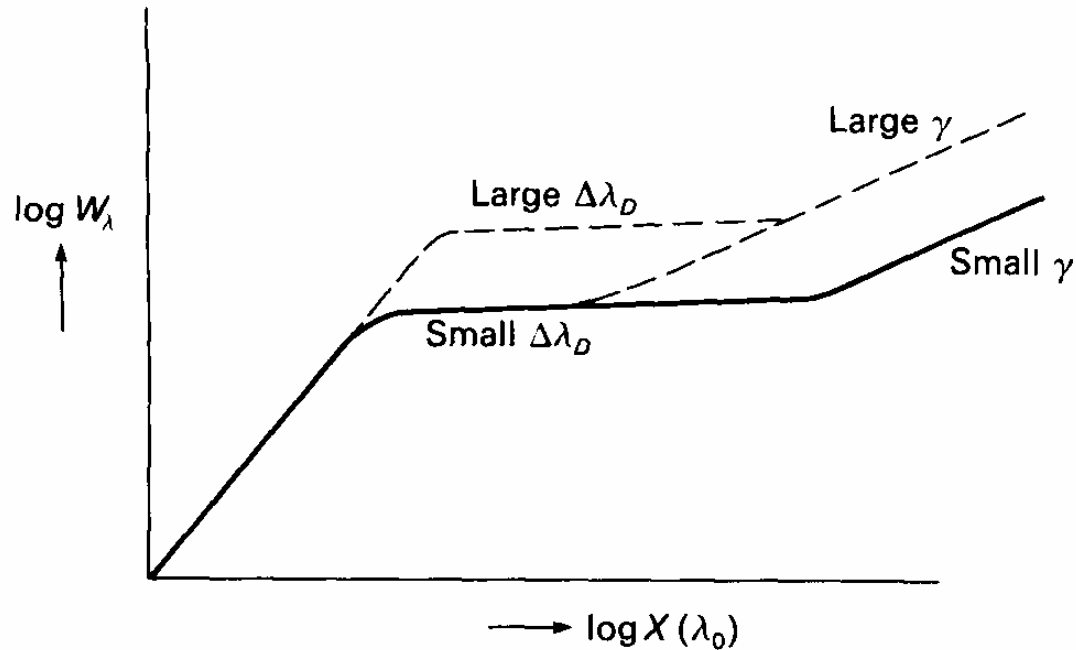
By superimposing natural and Doppler broadening, we obtain the overall behavior of W_λ with $N \cdot f$, namely the so-called *curve of growth*.

This curve is composed by three parts :

- at low $N \cdot f$, the intensity is proportional to $N \cdot f$
- for intermediate values of $N \cdot f$, the center of the line is deep but the wings are relatively unimportant; the intensity remains almost constant for a range of $N \cdot f$, $W \approx \text{const}$
- for very large values of $N \cdot f$, the intensity increases with $\sqrt{N \cdot f}$

Summary of overall effect on $W_\lambda - 2$

The curve of growth



The cross-over between the 3 regimes depends on the relative importance of the broadening mechanisms.

Doppler broadening is sensitive only to temperature, but collisions are sensitive also to density (or pressure).

A more precise theory

A more precise theory shows that the proper variables to be used are, for the ordinate:

$$(W_\lambda / \lambda) \left(c / \sqrt{2kTM + \langle v_{\text{vert}} \rangle^2} \right)$$

and for the abscissa:

$$Nf(\lambda / 5000) p$$

where W_λ and λ are both in Angstroms, c is the velocity of light, M is the mass of the atom, $\langle v_{\text{vert}} \rangle$ is the most probable value of the random *vertical* velocities, and p is a factor that allows for the variation with λ of the continuous absorption coefficient κ_λ .

Other effects influencing W_λ

Collisional (or pressure) broadening must be discussed in greater detail.

Indeed, for H the previous considerations on the curve of growth are incapable of explaining the observed profiles, so we must resort to a more complete discussion (*linear Stark effect, see later*).

Similar difficult problems are caused by the *Zeeman effect* in sunspots or magnetic stars. Magnetic fields split magnetically sensitive lines: at optical wavelengths the splitting often is seen only as line broadening, towards the IR the splitting becomes more noticeable since it increases as λ^2 , versus λ for Doppler broadening.

Some stars display orderly *currents* in their atmospheres. There might be other motions in stellar atmospheres, operating on microscopic (*microturbulence*) and macroscopic (*macroturbulence*) scales.

Collisional (pressure) broadening - 1

Charges passing near the radiating atom or ion cause *microscopic electric fields*. These short-lived fields of random direction and amplitude are sufficient to perturb the energy levels (*especially the outer ones*) of the ion. Therefore these collisions *alter the energy levels* of atoms and molecules, and the wavelengths of the corresponding transitions.

A general treatment is very difficult; interactions can cause not only line broadening, but also line *shifts* and *asymmetries*, which are not considered here.

The energy perturbations caused by collisions can be classified into 4 different interactions, whose dependence from the distance R from the radiating atom (or molecule) to the perturbing charge is of the type R^{-n} :

- $n = 2$, linear Stark, affecting H, typical perturbers are electrons and protons,
- $n = 3$, resonance broadening, rarely seen in stars,
- $n = 4$, quadratic Stark, most lines in hot stars, typical perturbers are electrons,
- $n = 5$, Van der Waals, most lines in cool stars, typical perturbers are H atoms.

Collisional (pressure) broadening - 2

A good example of collisionally broadened line profile is provided by the *H and K line of Ca II* in the solar photosphere.

In most stellar types, the broadening due to *collisions* is much larger than that due to the natural width, *however the resulting profile is the same of natural broadening, namely a Lorentz function, so the damping constants add together*. Due to this shape, *collisional damping contributes more to the wings of the line* (same as natural broadening), while Doppler broadening is more efficient at the center of the line, as already discussed.

A remarkable difference between natural and pressure broadening is that the *latter depends on the optical depth inside the stellar atmosphere, and therefore on temperature and density*.

In the hottest stars, the fastest particles are *free electrons*, so that the broadening is proportional to the *electron pressure P_e* .

In the cooler stars, the great majority of particles is constituted by neutral H atoms, whose density is proportional to the *gaseous pressure P_g* .

Stark effect for H and hydrogenic ions -1

The effect of electric interactions is particularly important for H (and so also for hydrogenic ions), but also difficult to discuss. The main reason is the degeneracy of the H energy levels, which increases with n^2 . The perturbation matrix elements is thus divided by numbers approaching zero, so that the effect becomes very large (linear Stark effect). The lines of heavier elements show instead a much smaller *quadratic Stark effect*.

Due to the dependence by n^2 , the broadening increases toward the head of the series, e.g. of the Balmer lines.

The effect contributes to the different aspect of the lines between dwarfs, giants and supergiants. In the dwarfs, the density is higher, so that the Stark effect is strong. In the giants and supergiants, the density is decidedly lower, and the broadening is essentially Doppler.

Stark effect for H and hydrogenic ions -2

The level n_s for which the lines merge together is connected to the electron density by means of the Inglis – Teller formula:

$$\log N_e = 22.0 - 7.0 \log n_s$$

which is quite evident in the spectrum of the A stars.

Macroscopic Stark effect

On the Sun, the high spatial resolution than can be achieved even from the ground, allows the detection of macroscopic electric fields, well ordered over lengths of several hundred km although of short temporal duration, in particular in proximity of dark spots at the moment of a magnetic polarity inversion producing a flare.

The spectral lines are separated into components by this *macroscopic Stark effect*, and the different components are *differently polarized*.

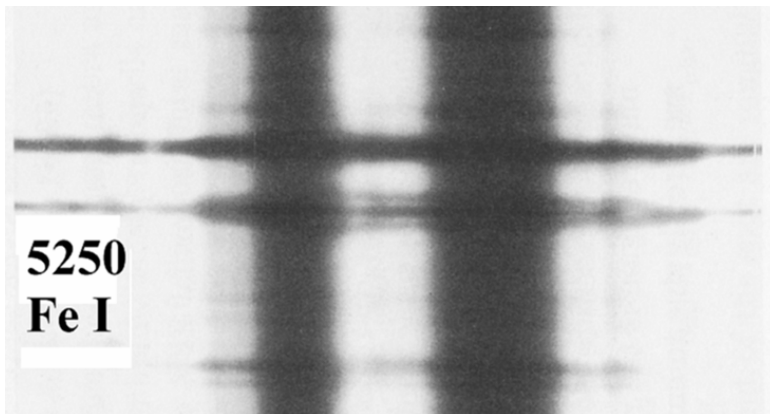
The Zeeman effect

A macroscopic magnetic field produces the Zeeman effect, well observable on the Sun especially in proximity of the dark spots.

The lines, especially those of particular metals, become separated in different components having different polarization.

In a generic star, the varying direction of the magnetic field along the line of sight usually prevents the resolution of the different components, and the Zeeman effect is seen as *a broadening of the line*.

The magnetic field can be very strong on peculiar stars and on white dwarfs, reaching intensities of several MegaGauss.



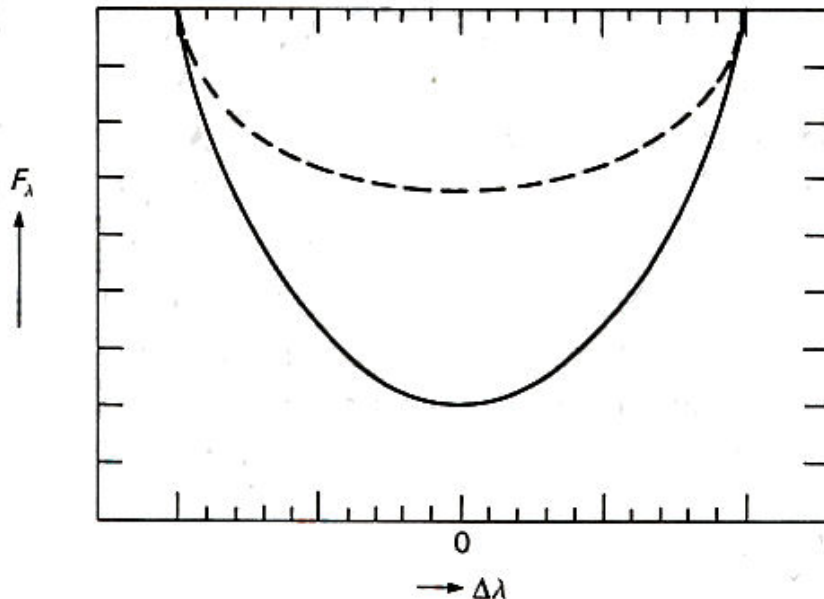
The Zeeman effect in a large solar dark spot affects the Fe I line at 5250Å. The splitting of 0.12Å corresponds to 3600 gauss. The field is almost as strong in the penumbra (center) than in the umbra (the two vertical dark streaks).

Rotational broadening

Thermal broadening describes the *microscopic* motion of individual particles in the atmosphere. The other extreme is *macroscopic* broadening of the lines caused by the *rotation of the whole star*.

Stellar rotation causes a characteristic broadening of the profiles, but it *does not affect the curve of growth*.

The generally unknown inclination i permits the measurement of $V_{\text{rot}} \cdot \sin i$ only, except for *eclipsing binaries*.



The figure shows a spectral line broadened by rotation. *The line profile is elliptical*, and depends from the limb darkening (dotted profile = no darkening, continuous line = strong darkening).

$$V_{\text{rot}} \sin i$$

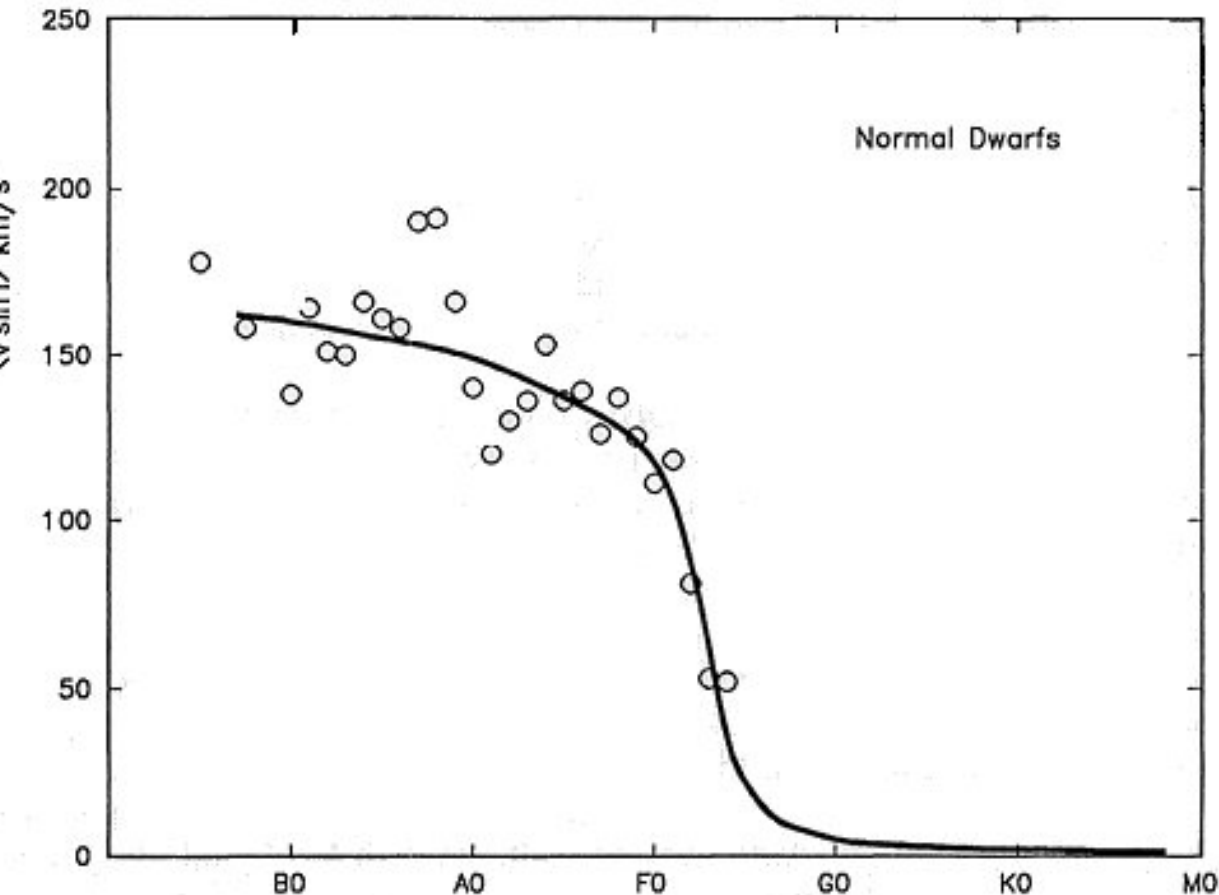
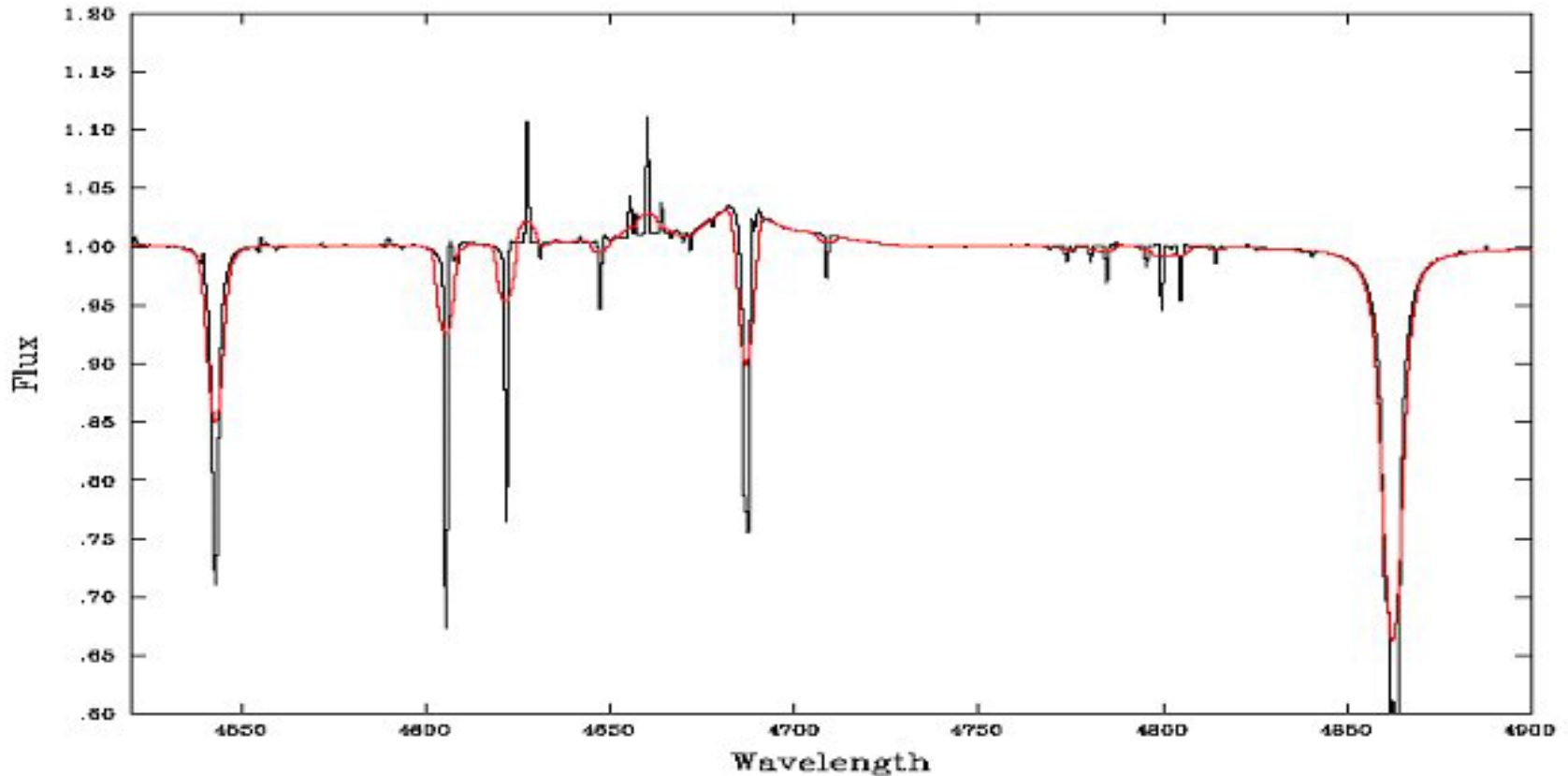


Fig. 17.16. The average rotation rates are shown for spectral intervals as a function of spectral type. (Data are from Uesugi and Fukuda (1982), Soderblom (1983), and Gray (1982b, 1984b).)

Many early-type ***OB stars*** are observed to be rotating rapidly, such that this is the major broadening mechanism.

Stars cooler than F0, for instance the Sun, are much slower rotators.

An overall example



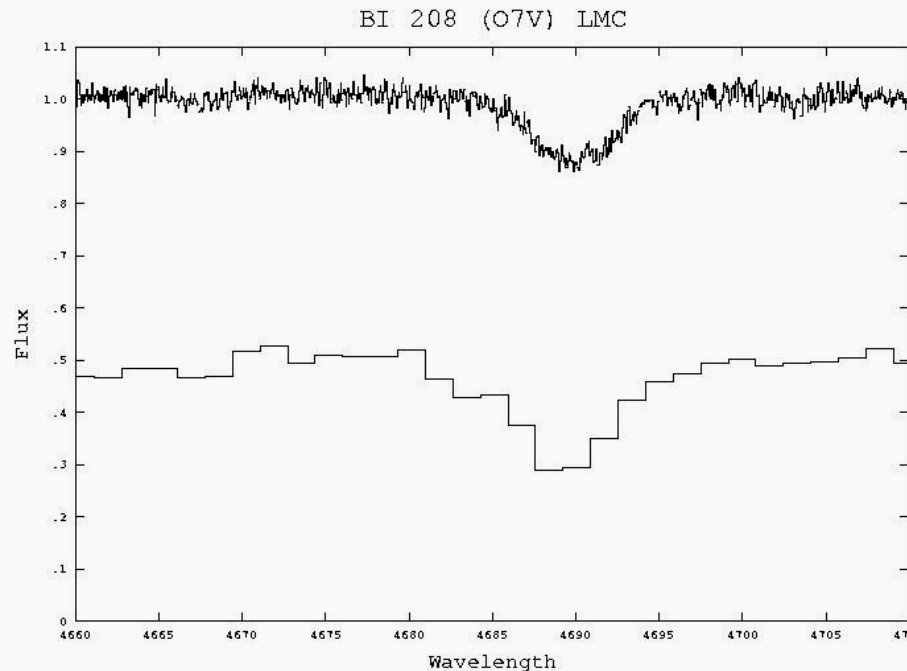
The figure shows a synthetic model of an O2 giant allowing for Doppler plus Stark broadening (**black**) plus a $V_{\text{rot}} \cdot \sin i = 200 \text{ km/s}$ rotational broadening applied (**red**).

Instrumental Broadening

Any spectrograph has a finite *resolution*, regardless of the sharpness of the spectral line. For low dispersion data, necessary when observing faint objects, this affects the observed line profile more than everything else. Stars with intrinsically narrow lines are generally broadened the most by the spectrograph.

In addition to defects of resolution, spectrographs might *scatter* light into absorption regions, again with appreciable effects on the determination of W .

Spectroscopy of HeII 4686 line in an **O** **star** in the Little Magellanic Cloud ($V = 14$). Contributions from Doppler thermal, linear Stark pressure, and rotational broadening are all present. At the top is a very high resolution spectrum from ESO 8m telescope in Chile, versus an intermediate resolution spectrum at bottom.



The line transfer equation - 1

Here, we follow the notation of Gray (see References), slightly different from that of our Chapter on Stellar Atmospheres; see also the .doc file).

The basic equation of radiation transfer is the same as for the continuum. However, it is better to consider separately the absorption and emission coefficients (here, per unit mass), and the source functions.

With l we indicate variables proper for the lines, and with c those for the continuum:

$$d\tau = (l + \kappa)\rho dx \quad , \quad S = \frac{j^l + j^c}{l + \kappa} = \frac{S_l + (\kappa/l)S_c}{1 + (\kappa/l)},$$

$$I(0) = \int_0^{\infty} S(\tau) e^{-\tau/\mu} d\tau / \mu \quad , \quad \pi F(0) = 2\pi \int_0^{\infty} S(\tau) E_2(\tau) d\tau$$

where E_2 is the *exponential integral* of order 2. The central problem is the same as for the continuum, how to obtain $S(\tau)$ in order to determine the exit flux $F(0)$. Notice that for the lines, τ *will vary with frequency (or wavelength) more rapidly than for the continuum.*

The line transfer equation - 2

As done in Chapter 2, assume a definite linear relationship between S and τ :

$$S(\tau) \approx \frac{3}{4\pi} F(0) \left[\tau + \frac{2}{3} \right] \quad \Rightarrow \quad S(\tau = (4\pi - 2) / 3) = S(\tau \approx 3.5) = F(0)$$

As already discussed at the beginning, τ is close to 3.5 higher up in the atmosphere for the core of the line, for progressively deeper layers in the wings. So we can conclude (always with some approximation), that there is a mapping between S as function of τ and $F(0)$ as function of ν (or λ): *the line profile maps the source function S at different depths.*

A great complication arises from Doppler, micro- and macro-turbulent motions, so that the previous conclusion cannot be entirely true: a whole *range of depths* will contribute to $F_\lambda(0)$

The abundance dependence - 1

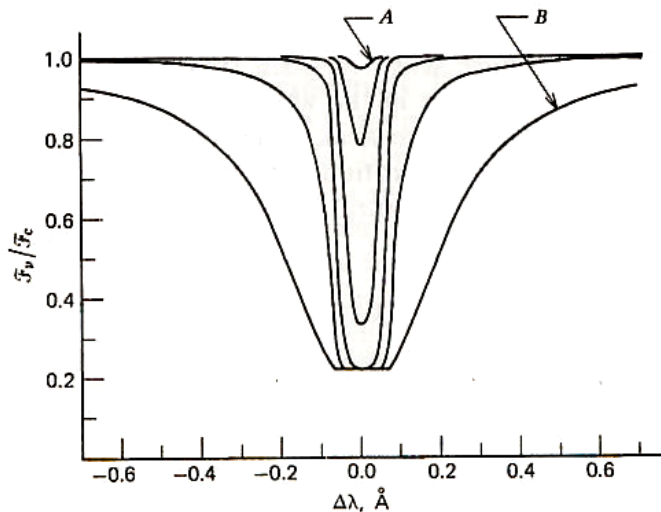
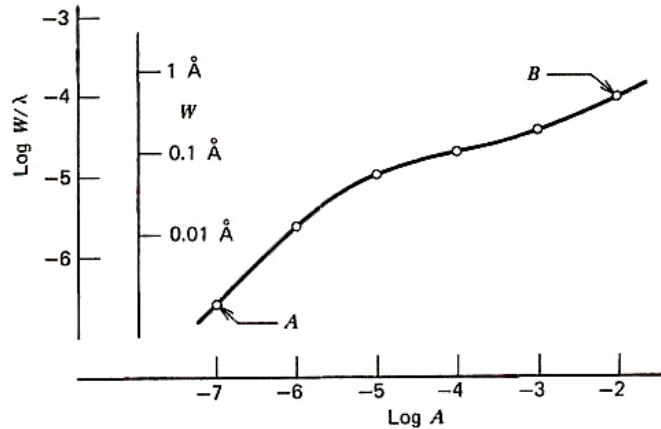


Fig. 13.12. Both the equivalent width (top) and the profile (bottom) change with chemical abundance of the absorbing species. The circles on the curve of growth correspond to the profiles below. Model has $S_0 = 0.87$ and $\log g = 4.0 \text{ cm/s}^2$.

Let us recall a curve of growth, as in the figure. This is typically a log-log plot of W vs. abundance (notice though that the ordinate is W/λ , because this choice normalizes Doppler dependent phenomena). Both the curve of growth and the line profile change with the abundance of this element **E**.

The abundance dependence - 2

We have already commented (in a very simplified way) the influence of *temperature and pressure* on the curve of growth of a specific line (we assume to know the value of the corresponding f). Here, we discuss the influence of the *abundance* of a given element E , indicated with A = percentage of E with respect to Hydrogen.

From the previous considerations, we expect that at small equivalent widths the line profile is dominated by the Doppler core, and the depth grows in proportion to A .

When the line wings become significant and the core saturates, then we have a regime of the order $A^{1/2}$.

At intermediate regimes (the core approaching saturation) the profile is essentially independent from A .

Notice that these conclusions could be reached analytically from the simple model of gas in a box, as in Chapter 2. The reality is much more complex, however the *basic shape of the curve of growth can be intuitively understood by this way.*

The abundance dependence - 3

These plots have the interesting property of being *scalable by a simple translation*: lines of the same element E (same A throughout the atmosphere) will differ only in *displacement along the abscissa* according to the different g , f and λ (better yet, to their product $gf\lambda$), different excitation energy χ , and absorption coefficient κ .

Assuming that all lines of a given element have the same curve of growth, we can derive by translation of all these curves into a theoretical one (which depends on the assumed model, e.g. LTE, pressure, temperature, microturbulence, etc.) the abundance of E .

As is generally always true, *differential methods* are surer than absolute ones:

therefore, it is easier to determine *difference of abundances* between stars having approximately similar spectra than the absolute values of their chemical composition.

Examples connected with solar Na-D

The solar profile of NaD

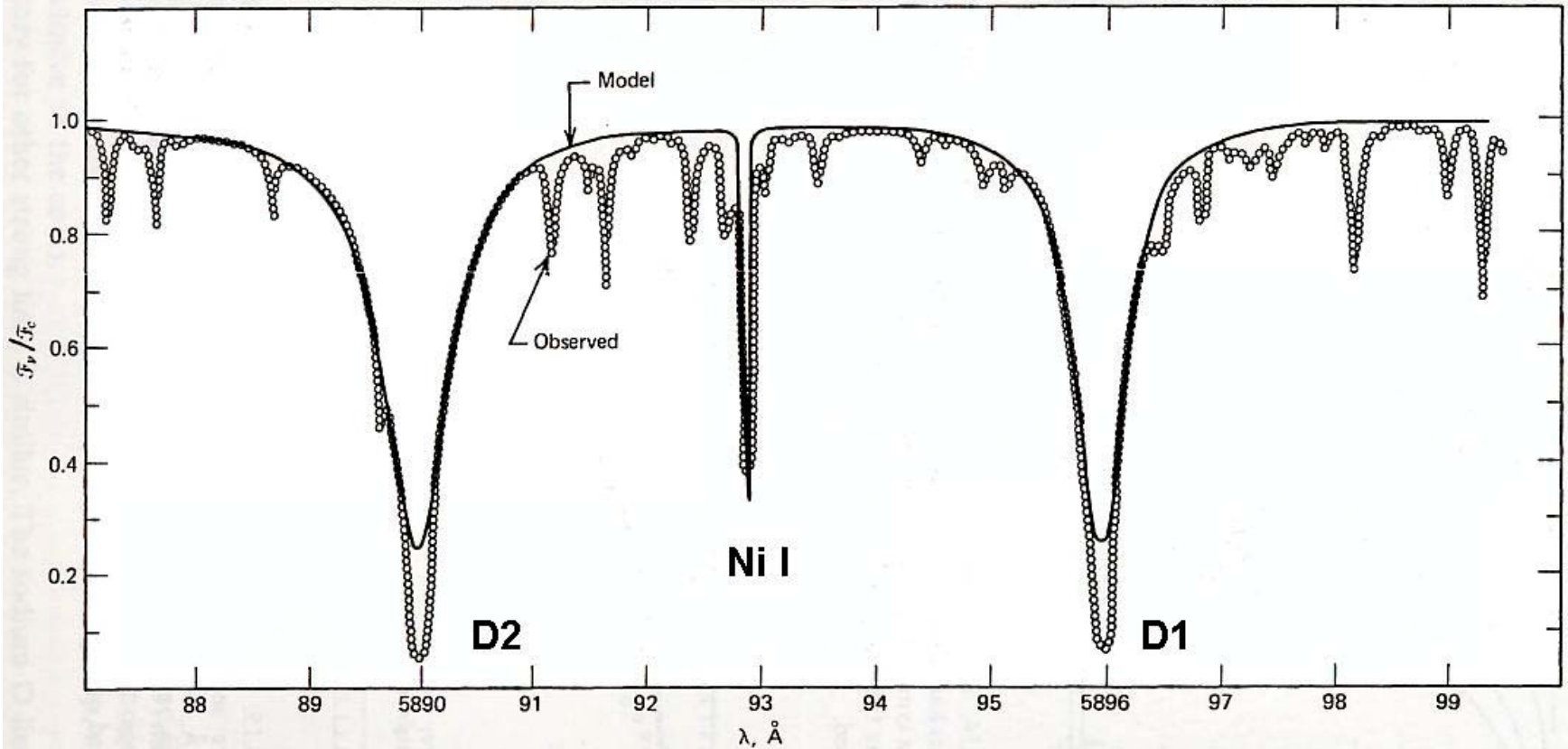
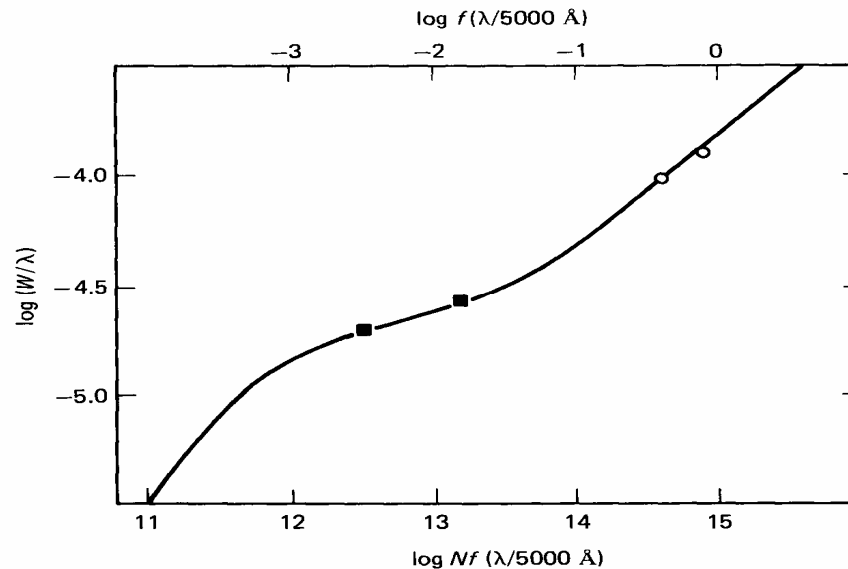


Fig. 13.16. Observations of the solar sodium D lines are compared with an LTE model. Serious discrepancies are seen in the cores. Almost all the weaker lines arise from telluric water vapor. (Observations courtesy of Kitt Peak National Observatories.)

1 - The curve of growth of NaI in the Sun



The solid curve is the theoretical curve of growth for the sun, W the equivalent width and λ the wavelength (both in \AA). N is the number of atoms in the lower level of the transition (capable of absorbing the line in question), and f the oscillator strength. Squares denote the observed points for the 3300 and circles for the 5890 doublets of NaI. We derive several conclusions:

1 - By comparing the horizontal upper scale with the lower one, we see that $\log_{10} N = 14.98$, $N \approx 1 \times 10^{15}$, which is the number of Na I atoms in the **lowest energy level**.

2 - The quantity of Na in the solar atmosphere

2 - On the other hand, $T = 5800$ K, and the electronic pressure P_e is approximately 10 barye; therefore from Saha equation we estimate that $N(\text{Na I})/N(\text{Na}_{\text{total}}) \approx 4.1 \times 10^{-4}$: essentially all Na in the solar photosphere *is ionized*, the very strong Na I D-doublet is indeed due to *a minute fraction of the element*; the strong lines of Na II are in the UV region.

3 - The real amount of Na atoms is therefore $N(\text{Na}_{\text{total}}) \approx 2 \times 5 \times 10^{18} \text{ cm}^{-2}$, and multiplying by the mass of the Na atom ($\approx 3.8 \times 10^{-23} \text{ g}$), we get a total mass in Na of approximately $0.094 \text{ mg} \cdot \text{cm}^{-2}$ in the unitary column extending through the photosphere, a very small quantity indeed!

3 – The optical depth of the NaD lines

Many of the strongest lines in the spectrum are *multiplets* with small separations.

One can easily measure the relative intensities of the two lines.

If the lines are weak, their relative intensities are given by the atomic constants.

If the lines are strong, they provide indications on the optical depth.

A good example is the NaD at 5890/96. The ratio of the statistical weights is 1:2 (same as for H and K of CaII), as observed for optically thin gases.

For an appreciable optical depth, we have:

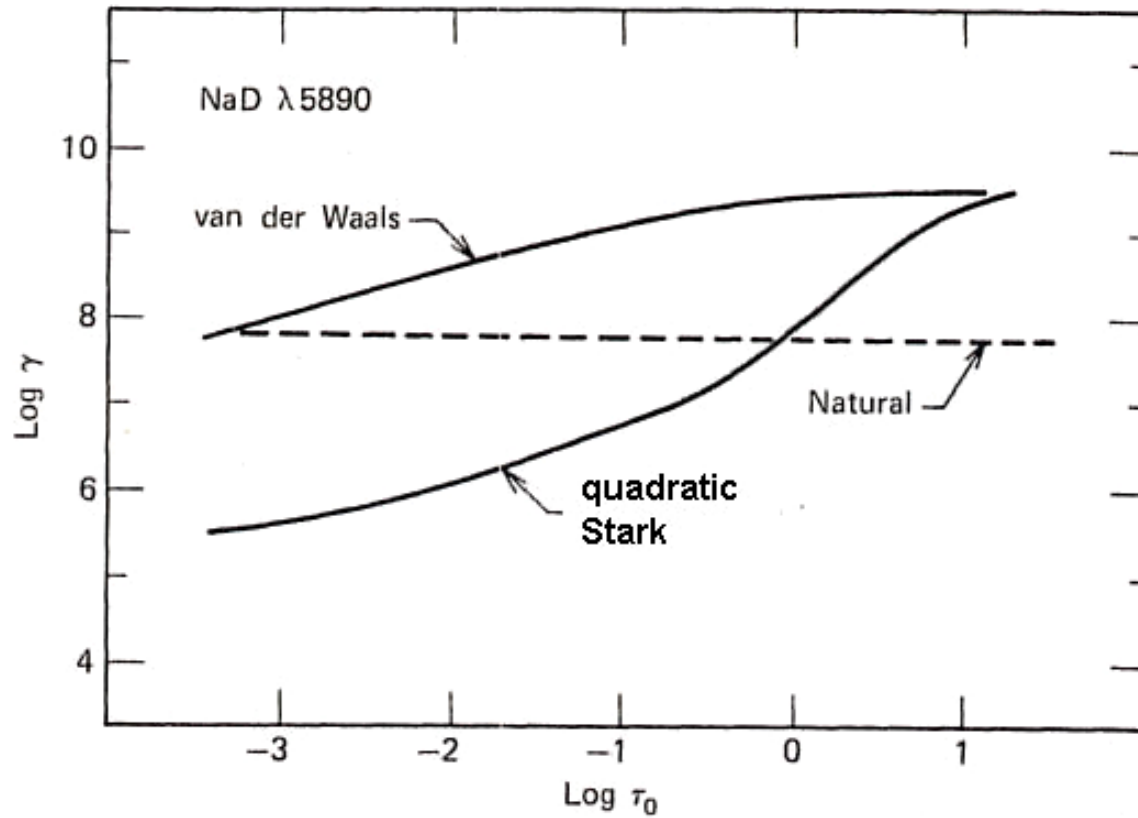
$$R = \frac{I(D2)}{I(D1)} = \frac{S_2(1 - e^{-2\tau})}{S_1(1 - e^{-\tau})} \quad (\mathcal{S} = \text{source function})$$

In the photosphere, the optical depth is very large, and the central intensities of two lines practically equal.

However, the wings will be sensitive to the optical depth, so we can estimate from *R in the wings* the number of atoms at the different optical depths. With the assumption $\mathcal{S}_1 = \mathcal{S}_2$, the wing profile also maps the source function with τ .

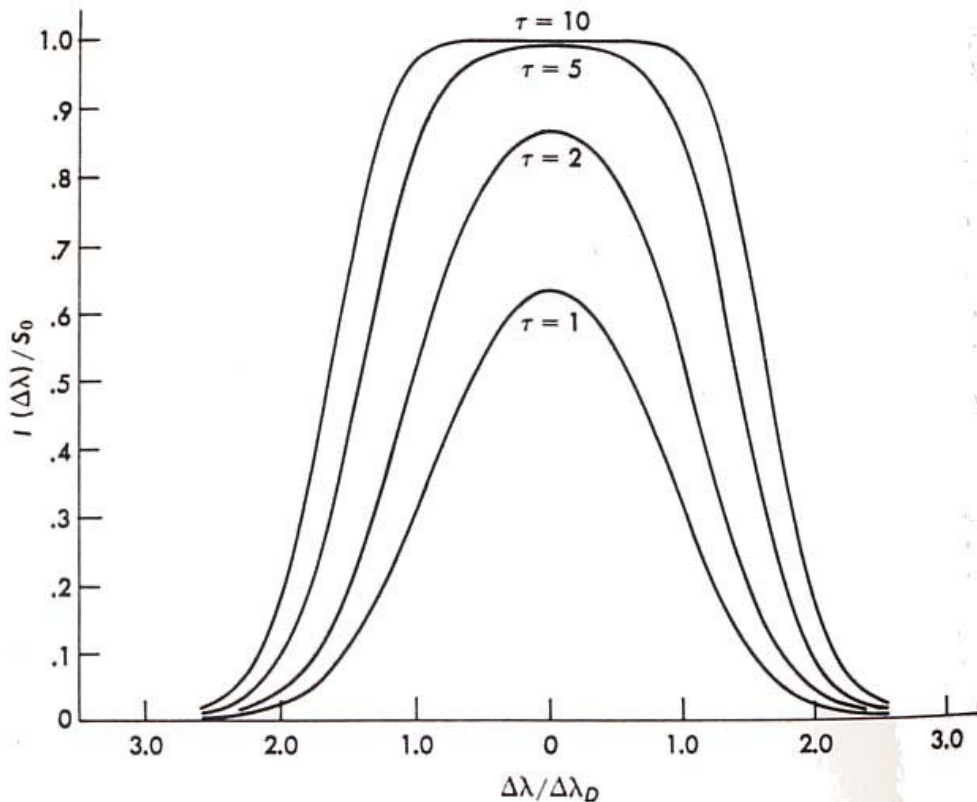
Obviously, the process can be generalized to other doublets.

4 - Broadening mechanisms for NaD



For NaD, natural broadening remains always smaller than van der Waals and quadratic Stark, which in turn are smaller than Doppler.

5 - Pure Doppler Broadening



A strong emission (or absorption) line, such as NaD, with pure Doppler (no natural) broadening and constant source function S , with increasing optical depth. Ordinate: intensity normalized to source function.

Abcissa: fractional distance of the line from the central value. At the center top, the intensity value reaches the source function.

If natural damping was important, the wings would be much stronger.

The line profile of strong lines maps the source function with τ .